Field-induced magnetic dipolar interaction for general boundary conditions

Sheng-Wen Li (李圣文)[1] and Li-Ping Yang (杨立平)[2,*]

[1]*Center for Quantum Technology Research, and Key Laboratory of Advanced Optoelectronic Quantum Architecture and Measurements, School of Physics, Beijing Institute of Technology, Beijing 100081, China*

[2]*Center for Quantum Sciences and School of Physics, Northeast Normal University, Changchun 130024, China*

(Received 24 May 2021; revised 17 July 2021; accepted 4 October 2021; published 26 October 2021)

By properly considering the propagation dynamics of the dipole field, we obtain the full magnetic dipolar interaction between two quantum dipoles for general situations. With the help the Maxwell equation and the corresponding Green function, this result applies for general boundary conditions and naturally unifies all the interaction terms between permanent dipoles, resonant or nonresonant transition dipoles, and even the counter-rotating interaction terms altogether. In particular, we study the dipolar interaction in a rectangular three-dimensional cavity with discrete field modes. When the two dipoles are quite near to each other and far from the cavity boundary, their interaction simply returns the free-space result; when the distance between the two dipoles is comparable to their distance to the cavity boundary and the field mode wavelength, the dipole images and near-resonant cavity modes bring in significant changes to the free-space interaction. This approach also provides a general way to study the interaction mediated by other kinds of fields.

DOI: 10.1103/PhysRevA.104.043709

I. INTRODUCTION

Electric and magnetic dipolar interactions widely exist in many microscopic systems, such as a Josephson qubit interacting with dielectric defects [1–4], a nitrogen-vacancy (NV) interacting with the nuclear spins around it [5,6], and dipolar interactions in many chemical and biological molecules [7–9]. In principle, the electromagnetic interactions between particles are indirectly induced by their local interaction with the field. Thus, it is possible to engineer the dipolar interaction by properly controlling the mediating electromagnetic (EM) field [10–18].

But in the literature, the magnetic dipolar interaction between two quantum dipoles with distance R has three different descriptions.

(i) *Direct exchange*. In free space, the classical dipolar interaction between two static magnetic dipoles is ($\mathbf{e}_R$ is the unit directional vector of the distance R) [19]

$$V_0 = \frac{\mu_0}{4\pi R^3}[\vec{m}_1 \cdot \vec{m}_2 - 3(\vec{m}_1 \cdot \mathbf{e}_R)(\vec{m}_2 \cdot \mathbf{e}_R)], \tag{1}$$

and thus the quantum dipolar interaction is usually obtained by simply replacing the classical dipole moments with quantum operators $\hat{\mathbf{m}}_i$. Here the mediation effect of the EM field is not explicit, and the frequencies of the quantum dipoles do not appear [5,6,20] .

(ii) *Master equation correction.* The dynamics of two dipoles weakly interacting with the EM field can be described by a Markovian master equation, where the system Hamiltonian contains an interaction correction $\hat{V}_{12} = V(\omega)\,\hat{\tau}_1^+\hat{\tau}_2^- + \text{H.c.}$, where $\hat{\tau}_{1,2}^{\pm}$ are the transition operators, and [21–24]

$$V(\omega) = \frac{\mu_0}{4\pi R^3}\left\{\vec{m}_1 \cdot \vec{m}_2[(1-\eta^2)\cos\eta + \eta\sin\eta] - 3(\vec{m}_1 \cdot \mathbf{e}_R)(\vec{m}_2 \cdot \mathbf{e}_R)\left[\left(1-\frac{\eta^2}{3}\right)\cos\eta + \eta\sin\eta\right]\right\}. \tag{2}$$

Here $\eta := \omega R/c$, and ω is the transition frequency of the two resonant dipoles. The interaction strength $V(\omega)$ exhibits an oscillating decay with the distance R and returns Eq. (1) when $\omega R/c \to 0$. However, since the rotating-wave approximation (RWA) must be applied in a tricky way when deriving this master equation, this approach could only give the interaction term between two resonant transition dipoles with equal frequencies, while the other interaction terms cannot be obtained, e.g., those between nonresonant dipoles [25], permanent dipoles, and the counter-rotating terms. Besides, this approach cannot be applied when the field modes are discrete, e.g., in an ideal lossless cavity.

(iii) *Mode elimination.* Considering the two dipoles (frequency $\omega_{1,2}$) both interacting with one common field mode (frequency ν), e.g., $\hat{V} = \hat{a}^\dagger(g_1\hat{\tau}_1^- + g_2\hat{\tau}_2^-) + \text{H.c.}$, the mediating field mode can be eliminated by the Fröhlich-Nakajima transform [10,26–29], which gives $\hat{V}_{12} \simeq \tilde{\beta}\,\hat{\tau}_1^+\hat{\tau}_2^- + \text{H.c.}$, with (see Appendix A)

$$\tilde{\beta} = \frac{1}{2}\left[\frac{g_1 g_2^*}{\omega_1 - \nu} + \frac{g_2 g_1^*}{\omega_2 - \nu}\right]. \tag{3}$$

In more realistic cases, usually more field modes should be involved.

These approaches are not always equivalent to each other, with different application conditions, and it is not quite clear

*yanglp710@nenu.edu.cn

how these approaches are connected with each other. In this paper, we make a general approach which unifies all the above results together in the same framework. The existence of one dipole would generate a dipole field propagating to the other one, and then the dipolar interaction would be generated [30,31]. The dynamics of this dipole field is given by the Maxwell equation and the corresponding Green function [14–16,32,33]. Based on this idea, we obtained the full dipolar interaction for two quantum magnetic dipoles for general boundary conditions. Our result naturally includes all the interaction terms between permanent dipoles, resonant or nonresonant transition dipoles, and even the counter-rotating interaction terms altogether [31]. These terms are crucial for the delicate control in microscopic systems under the proper driving field, especially for magnetic dipolar interactions, since one magnetic dipole operator usually contains both nonzero transition and permanent dipole moments. Under proper conditions, our result well reduces to all the above three cases.

In particular, we study the dipolar interaction between two magnetic dipoles inside a rectangular three-dimensional (3D) cavity made of ideal conductors, where the field modes are fully discrete. It turns out, when the two dipoles are quite near to each other and far from the boundaries, the interaction always returns to the static dipolar interaction (1) in free space; when the dipoles are close to the cavity boundary, the dipole field propagation is strongly restricted due to the conductor boundary, which further influences the dipolar interaction generated.

The paper is arranged as follows. In Sec. II, we show the derivation for the dipolar interaction for general situations. In Sec. III, we study how the Green function is evaluated in a rectangular 3D cavity. In Sec. IV, we show the numerical results for the dipolar interaction. In Sec. V, we discuss the possible application of these results in different physical systems.

II. DIPOLE FIELD PROPAGATION

We consider that two magnetic dipoles are placed in the EM field. The Hamiltonian of each dipole is $\hat{H}_\alpha = \sum_u E_u^{(\alpha)} |u\rangle_\alpha\langle u|$, where $E_u^{(\alpha)}$and $|u\rangle_\alpha$ are the eigenenergy and the corresponding eigenstate of dipole-α ($\alpha = 1$ and 2).

The two magnetic dipoles interact with the EM field via their local interactions $\hat{V}_\alpha = -\hat{\mathbf{m}}_\alpha \cdot \hat{\mathbf{B}}(\mathbf{r}_\alpha)$, where $\mathbf{r}_\alpha$ is the position of dipole-α, and $\hat{\mathbf{m}}_\alpha := \sum_{uv} \vec{m}_\alpha^{uv} \hat{\tau}_\alpha^{uv}$ is the dipole operator, with $\vec{m}_\alpha^{uv} := \langle u|\hat{\mathbf{m}}_\alpha|v\rangle_\alpha$ and $\hat{\tau}_\alpha^{uv} := |u\rangle_\alpha\langle v|$ (see Fig. 1). Usually, one dipole operator $\hat{\mathbf{m}}_\alpha$ contains both nonzero permanent dipoles (the diagonal terms $\vec{m}_\alpha^{uu}|u\rangle_\alpha\langle u|$) and transition dipoles (the off-diagonal terms $\vec{m}_\alpha^{uv}|u\rangle_\alpha\langle v|$ with $u \neq v$) together [30]. Hereafter, these vector operators are denoted as $\vec{m}_\alpha^{uv}|u\rangle_\alpha\langle v| := \hat{\mathbf{m}}_\alpha^{uv}$, and thus $\hat{\mathbf{m}}_\alpha = \sum_{uv} \hat{\mathbf{m}}_\alpha^{uv}$.

The existence of one magnetic dipole changes the EM field dynamics, and when such field changes propagate to the other dipole, the interaction is generated between the two dipoles [30,31]. Here we first consider the dipole field generated by dipole-1 interacting with dipole-2. Notice that the quantized magnetic field $\hat{\mathbf{B}}(\mathbf{r}, t)$ also follows the Maxwell equation (Appendix B)

$$\left[\tfrac{1}{c^2}\partial_t^2 - \nabla^2\right]\hat{\mathbf{B}}(\mathbf{r}, t) = \mu_0 \nabla \times \hat{\mathbf{J}}_1(\mathbf{r}, t), \tag{4}$$

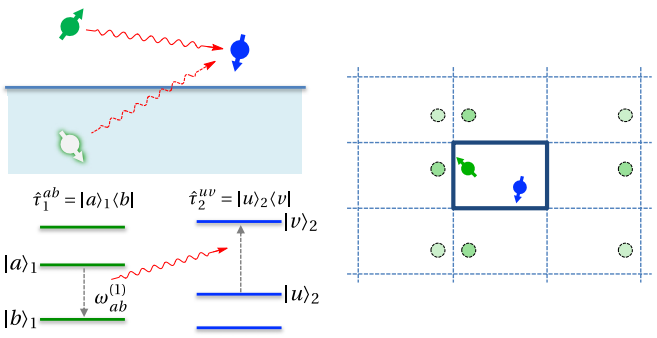

FIG. 1. Demonstration for the dipole field propagation and the image sources.

which has the same form as the classical one [19,34–37], although the explicit form of the quantized field $\hat{\mathbf{B}}(\mathbf{r}, t)$ is not written down. Here $\hat{\mathbf{J}}_1 := \nabla \times \hat{\mathbf{M}}_1$ is the electric current density induced by dipole-1, and $\hat{\mathbf{M}}_1(\mathbf{r}, t) := \hat{\mathbf{m}}_1(t)\,\delta(\mathbf{r} - \mathbf{r}_1)$ is the magnetization density.

The dynamics of the quantized field contains two contributions, $\hat{\mathbf{B}}(\mathbf{r}, t) = \hat{\mathbf{B}}_0(\mathbf{r}, t) + \hat{\mathbf{B}}_{\rm d1}(\mathbf{r}, t)$, where $\hat{\mathbf{B}}_0(\mathbf{r}, t)$ comes from the vacuum EM field, given by the homogenous equation $[c^{-2}\partial_t^2 - \nabla^2]\hat{\mathbf{B}}_0 = 0$, and $\hat{\mathbf{B}}_{\rm d1}(\mathbf{r}, t)$ is the dipole field generated by dipole-1, which can be given with the help of the tensor Green function [32,38,39],

$$\hat{\mathbf{B}}_{\rm d1}(\mathbf{r}, t) = \mu_0 \int_{-\infty}^{\infty} dt' \int_V d^3r'\, \mathbb{G}_{\rm m}(\mathbf{r}t, \mathbf{r}'t') \cdot \hat{\mathbf{J}}_1(\mathbf{r}', t'),$$
$$\left[\tfrac{1}{c^2}\partial_t^2 - \nabla^2\right]\mathbb{G}_{\rm m}(\mathbf{r}t, \mathbf{r}'t') = \nabla \times \mathbb{I}\,\delta(\mathbf{r} - \mathbf{r}')\delta(t - t'). \tag{5}$$

Here $\mathbf{r}$ ($\mathbf{r}'$) denotes the field (source) position in the Green function $\mathbb{G}_{\rm m}(\mathbf{r}t, \mathbf{r}'t')$.

In the above dipole field $\hat{\mathbf{B}}_{\rm d1}(\mathbf{r}, t)$, the dynamics of dipole-1 is contained in the current $\hat{\mathbf{J}}_1(\mathbf{r}, t) = \nabla \times [\hat{\mathbf{m}}_1(t)\delta(\mathbf{r} - \mathbf{r}_1)]$. Here we make an approximation that, during the field propagation time ($\sim R/c$), the dynamics of dipole-1 can be regarded as only governed by its self-Hamiltonian $\hat{H}_1$ and thus follows the unitary evolution, which gives $\hat{\mathbf{m}}_\alpha^{ab}(t') \simeq \hat{\mathbf{m}}_\alpha^{ab}(t)\,\exp[-i\omega_{ab}^{(\alpha)}(t' - t)]$, with $\hbar\omega_{ab}^{(\alpha)} := E_a^{(\alpha)} - E_b^{(\alpha)}$ [30,31]. In most microscopic experiments, the distance between different dipoles are within several microns; thus, the propagation time for their interactions ($R/c \lesssim 10^{-15}$ s) is much shorter than the decay time of each single dipole, which guarantees this approximation is reliable. Then the dipole field (5) can be further obtained as

$$\begin{aligned}\hat{\mathbf{B}}_{\rm d1}(\mathbf{r}, t) &= \mu_0 \int_{-\infty}^{\infty} dt' \int_V d^3r'\, \tilde{\mathbb{G}}_{\rm m}(\mathbf{r}t, \mathbf{r}'t') \cdot \nabla' \\ &\quad \times [\hat{\mathbf{m}}_1(t')\delta(\mathbf{r}' - \mathbf{r}_1)] \\ &\simeq -\mu_0 \sum_{ab} \int_{-\infty}^{\infty} dt' \int_V d^3r'\, \tilde{\mathbb{G}}_{\rm m}(\mathbf{r}t, \mathbf{r}'t') \cdot \nabla_1 \\ &\quad \times \left[\hat{\mathbf{m}}_1^{ab}(t) e^{-i\omega_{ab}^{(1)}(t'-t)}\delta(\mathbf{r}' - \mathbf{r}_1)\right] \\ &= \mu_0 \sum_{ab} \tilde{\mathbb{G}}_{\rm m}\left(\mathbf{r}, \mathbf{r}_1; \omega_{ab}^{(1)}\right) \times \overleftarrow{\nabla}_1 \cdot \hat{\mathbf{m}}_1^{ab}(t). \end{aligned} \tag{6}$$

Here $[\mathbb{G} \times \overleftarrow{\nabla}]_{ij} := \epsilon_{jpq}\partial_q \mathbb{G}_{ip}$ means the curl operation to the left, ∇'/∇_1 is the derivative with respect to $\mathbf{r}'/\mathbf{r}_1$, and

$$\tilde{\mathbb{G}}_{\rm m}(\mathbf{r},\mathbf{r}';\omega) := \int_{-\infty}^{\infty} dt'\, \mathbb{G}_{\rm m}(\mathbf{r}t,\mathbf{r}'t')e^{-{\rm i}\omega(t'-t)} \tag{7}$$

is the Fourier transform of the Green function $\mathbb{G}_{\rm m}(\mathbf{r}t,\mathbf{r}'t')$.

Therefore, the local interaction between dipole-2 (at position $\mathbf{r_2}$) and the dipole field $\hat{\mathbf{B}}_{\rm d1}(\mathbf{r},t)$ naturally gives the dipolar interaction as the following symmetric form:

$$\begin{aligned}\hat{V}_{2\leftarrow1} &= -\hat{\mathbf{m}}_2(t)\cdot\hat{\mathbf{B}}_{\rm d1}(\mathbf{r}_2,t)\\ &= \mu_0\sum_{ab,uv}\hat{\mathbf{m}}_2^{uv}\cdot\tilde{\mathbb{G}}_{\rm m}\big(\mathbf{r}_2,\mathbf{r}_1;\omega_{ab}^{(1)}\big)\times\overleftarrow{\nabla}_1\cdot\hat{\mathbf{m}}_1^{ab}\\ &= \mu_0\sum_{ab,uv}\hat{\mathbf{m}}_2^{uv}\cdot\nabla_2\times\tilde{\mathbb{G}}_{A}\big(\mathbf{r}_2,\mathbf{r}_1;\omega_{ab}^{(1)}\big)\times\overleftarrow{\nabla}_1\cdot\hat{\mathbf{m}}_1^{ab}.\end{aligned} \tag{8}$$

Here $\tilde{\mathbb{G}}_A(\mathbf{r},\mathbf{r}';\omega)$ is introduced from $\tilde{\mathbb{G}}_{\rm m}(\mathbf{r},\mathbf{r}';\omega) = \nabla\times\tilde{\mathbb{G}}_A(\mathbf{r},\mathbf{r}';\omega)$, which is the Green function for the vector potential $\mathbf{B} = \nabla\times\mathbf{A}$. And $\tilde{\mathbb{G}}_A(\mathbf{r},\mathbf{r}';\omega)$ follows

$$[\nabla^2 + (\omega/c)^2]\tilde{\mathbb{G}}_A(\mathbf{r},\mathbf{r}';\omega) = -\mathbb{I}\,\delta(\mathbf{r}-\mathbf{r}'). \tag{9}$$

The interaction (8) is gauge independent, since the term $\nabla\times\tilde{\mathbb{G}}_A$ in $\hat{V}_{2\leftarrow1}$ remains unchanged in gauge transformations. In addition, it is worth noting that the RWA is not needed throughout the above derivations.

Therefore, once $\tilde{\mathbb{G}}_A(\mathbf{r},\mathbf{r}';\omega)$ is solved, the dipolar interaction $\hat{V}_{2\leftarrow1}$ can be obtained from Eq. (8). The full dipolar interaction between the two magnetic dipoles also should involve the interaction between dipole-1 and the field induced from dipole-2, i.e.,

$$\begin{aligned}\hat{V}_{1\leftrightarrow2} &= \tfrac{1}{2}[\hat{V}_{2\leftarrow1}+\hat{V}_{1\leftarrow2}]\\ &= -\tfrac{1}{2}[\hat{\mathbf{m}}_2\cdot\hat{\mathbf{B}}_{\rm d1}(\mathbf{r}_2)+\hat{\mathbf{m}}_1\cdot\hat{\mathbf{B}}_{\rm d2}(\mathbf{r}_1)].\end{aligned} \tag{10}$$

In free space, the Green equation (9) has an isotropic solution: $\tilde{\mathbb{G}}_A(\mathbf{r}_2,\mathbf{r}_1;\,\omega\equiv ck) = (\cos kR/4\pi R)\,\mathbb{I}$, with $R\equiv|\mathbf{r}_2-\mathbf{r}_1|$. Then Eq. (8) gives the dipolar interaction as $\hat{V}_{2\leftarrow1} = \sum_{uv,ab}V_{2\leftarrow1}^{uv,ab}(\omega_{ab}^{(1)})\,\hat{\tau}_2^{uv}\hat{\tau}_1^{ab}$, where the interaction strength $V_{2\leftarrow1}^{uv,ab}(\omega_{ab}^{(1)})$ of each term is given by

$$\begin{aligned}V_{2\leftarrow1}^{uv,ab}(\omega) &= \mu_0\big[\vec{m}_2^{uv}\cdot\vec{m}_1^{ab}\nabla^2-(\vec{m}_2^{uv}\cdot\nabla)\big(\vec{m}_1^{ab}\cdot\nabla\big)\big]\frac{\cos kR}{4\pi R}\\ &= \frac{\mu_0}{4\pi R^3}\left\{\vec{m}_2^{uv}\cdot\vec{m}_1^{ab}\left[(1-\eta^2)\cos\eta+\eta\sin\eta\right]-3(\vec{m}_2^{uv}\cdot\mathbf{e}_{\rm R})\big(\vec{m}_1^{ab}\cdot\mathbf{e}_{\rm R}\big)\left[\left(1-\frac{\eta^2}{3}\right)\cos\eta+\eta\sin\eta\right]\right\},\end{aligned} \tag{11}$$

where $\eta = \omega R/c = kR$. This result has the same form as the master equation approach (2), and here $\hat{\mathbf{m}}_2^{uv}$ and $\hat{\mathbf{m}}_1^{ab}$ no longer need to be resonant dipoles.

The different matrix elements of the operator $\hat{V}_{2\leftarrow1}$ indicates different kinds of interactions. For example, considering each dipole only has two levels $|{\rm g}\rangle_\alpha$, $|{\rm e}\rangle_\alpha$ as the ground and excited states, the interaction term $\langle{\rm e_1g_2}|\hat{V}_{2\leftarrow1}|{\rm g_1e_2}\rangle\,|{\rm e_1g_2}\rangle\langle{\rm g_1e_2}| \equiv V_{2\leftarrow1}^{\rm ge,eg}(\omega_{\rm eg}^{(1)})\,\hat{\tau}_1^{+}\hat{\tau}_2^{-}$ gives the interaction between two transition dipoles ($\hat{\tau}_1^{+} = |{\rm e}\rangle_1\langle{\rm g}|$ and $\hat{\tau}_2^{-} = |{\rm g}\rangle_2\langle{\rm e}|$), which just returns Eq. (2); the interaction term $\langle{\rm e_1g_2}|\hat{V}_{2\leftarrow1}|{\rm e_1g_2}\rangle\,|{\rm e_1g_2}\rangle\langle{\rm e_1g_2}| \equiv V_{2\leftarrow1}^{\rm gg,ee}(\omega_{\rm ee}^{(1)}=0)\,\hat{\tau}_1^{\rm ee}\hat{\tau}_2^{\rm gg}$ indicates the interaction between two permanent dipoles, namely, when dipole-1 is in $|{\rm e}\rangle_1$ and dipole-2 is in $|{\rm g}\rangle_2$, which exactly returns the static dipolar interaction (1). Besides, $\hat{V}_{2\leftarrow1}$ also includes the interaction terms between one permanent dipole and one transition dipole, e.g., $V_{2\leftarrow1}^{\rm ee,eg}(\omega_{\rm eg}^{(1)})\,\hat{\tau}_1^{+}\hat{\tau}_2^{\rm ee}$, and counter-rotating terms such as $V_{2\leftarrow1}^{\rm eg,eg}(\omega_{\rm eg}^{(1)})\,\hat{\tau}_1^{+}\hat{\tau}_2^{+}$ [31]. Though usually neglected, these counter-rotating terms could exhibit significant physical effects under the proper driving field.

On the other hand, the interaction propagated from dipole-2 is $\hat{V}_{1\leftarrow2} = \sum_{uv,ab}V_{1\leftarrow2}^{ab,uv}(\omega_{uv}^{(2)})\,\hat{\tau}_1^{ab}\hat{\tau}_2^{uv}$, and the full interaction is $\hat{V}_{1\leftrightarrow2} = \frac{1}{2}(\hat{V}_{1\leftarrow2}+\hat{V}_{2\leftarrow1})$. Because of the isotropy of $\tilde{\mathbb{G}}_A(|\mathbf{r}_1-\mathbf{r}_2|\equiv R)$ in free space, we have $V_{1\leftarrow2}^{ab,uv}(\omega) = V_{2\leftarrow1}^{uv,ab}(\omega)$, except now the frequency is $\omega_{uv}^{(2)}$ from dipole-2. For the resonant case $|\omega_{ab}^{(1)}| = |\omega_{uv}^{(2)}|$, the interaction strengths contributed from both directions $1\leftarrow2$ and $2\leftarrow1$ are equal.

It is also worth noticing that the explicit form of the quantized field $\hat{\mathbf{B}}(\mathbf{r},t)$ is not needed throughout the above derivations, and the starting point is simply the Maxwell equation (4); thus, the above results do not depend on how the EM field is quantized (e.g., whether the Coulomb or the Lorenz gauge is used). The tensor Green function $\tilde{\mathbb{G}}_A(\mathbf{r},\mathbf{r}';\omega)$ is the same as the one in classical electrodynamics, and the results here apply for general boundary conditions.

III. THE DIPOLAR INTERACTION INSIDE A LOSSLESS CAVITY

Now we further consider the dipolar interaction between two dipoles inside a rectangular cavity, which is made of ideal conductors with no loss.

In this case, the field modes in the cavity are fully discrete. The above discussions about the dipole field propagation still holds, and the cavity boundary condition is naturally included in the tensor Green function $\tilde{\mathbb{G}}_A(\mathbf{r},\mathbf{r}';\omega)$ from Eq. (9), i.e.,

$$\hat{n}\times\tilde{\mathbb{G}}_A(\mathbf{r},\mathbf{r}';\omega) = 0, \quad \nabla\cdot\tilde{\mathbb{G}}_A(\mathbf{r},\mathbf{r}';\omega) = 0 \tag{12}$$

for $\mathbf{r}$ on the conductor plane [38,39]. Here the Green function can be written as $\tilde{\mathbb{G}}_A = G_A^x\,\mathbf{e}_x\mathbf{e}_x + G_A^y\,\mathbf{e}_y\mathbf{e}_y + G_A^z\,\mathbf{e}_z\mathbf{e}_z$, and the above boundary condition indicates $G_A^\sigma = 0$ on the sidewalls and $\partial_\sigma G_A^\sigma = 0$ on the end caps with respect to direction-σ (for $\sigma = x$, y, and z).

The Green function $\tilde{\mathbb{G}}_A(\mathbf{r},\mathbf{r}';\omega)$ has the following solution of mode expansion:

$$G_A^\sigma(\mathbf{r},\mathbf{r}';\omega) = \sum_{\mathbf{k}}\frac{\mathtt{A}_{\mathbf{k}}^\sigma(\mathbf{r})\mathtt{A}_{\mathbf{k}}^\sigma(\mathbf{r}')}{\mathbf{k}^2-(\omega/c)^2}, \tag{13}$$

where $\{\vec{\mathbf{A}}_{\mathbf{k}}(\mathbf{r})\}$ is a set of orthonormal eigenfunctions for $[\nabla^2+\mathbf{k}^2]\vec{\mathbf{A}}_{\mathbf{k}}(\mathbf{r})=0$, with $\mathbf{k}$ indexing the field modes (see Appendix C). Then the dipolar interaction can be further obtained [from Eq. (8)] as $\hat{V}_{2\leftarrow 1}=\sum_{uv,ab}V_{2\leftarrow 1}^{uv,ab}(\omega_{ab}^{(1)})\,\hat{\tau}_2^{uv}\hat{\tau}_1^{ab}$, and the interaction strength of each term is given by

$$V_{2\leftarrow 1}^{uv,ab}(\omega)=\sum_{\mathbf{k}}\frac{c^2\zeta_{2,\mathbf{k}}^{uv}\zeta_{1,\mathbf{k}}^{ab}}{\omega^2-c^2\mathbf{k}^2}\sim\sum_{|\mathbf{k}|\simeq\frac{\omega}{c}}\frac{c^2\zeta_{2,\mathbf{k}}^{uv}\zeta_{1,\mathbf{k}}^{ab}/2\omega}{\omega-c|\mathbf{k}|},\tag{14}$$

where $\zeta_{\alpha,\mathbf{k}}^{ab}:=\sqrt{\mu_0}\,\vec{\mathfrak{m}}_{\alpha}^{ab}\cdot\nabla\times\vec{\mathbf{A}}_{\mathbf{k}}(\mathbf{r}_\alpha)$ for $\alpha=1$ and 2.

Intuitively, since $\omega^2-c^2\mathbf{k}^2$ appears in the denominator, we may expect that only the near-resonant terms with $|\mathbf{k}|\simeq\omega/c$ dominate in the summation, and that would give an interaction strength returning the result (3) in the mode elimination approach (see Appendix A). However, it turns out the above summation series converges too slowly, since the density of state of the field modes also increases as $\sim\mathbf{k}^2$, which is in the same scale as the denominator $\omega^2-c^2\mathbf{k}^2$. As a result, only counting the near-resonant terms is not enough to give a precise evaluation for the dipolar interaction.

On the other hand, $G_A^{\sigma}(\mathbf{r},\mathbf{r}';\omega\equiv ck)$ also can be written down in the form of image expansion (Fig. 1), but that also has the slow-converging problem for numerical estimations. This problem can be solved by the improved Ewald expansion [38,39], that is, with the help of $\mathrm{erf}(x)+\mathrm{erfc}(x)=1$, the Green function is separated as $G_A^{\sigma}(\mathbf{r},\mathbf{r}';\omega)\equiv G_{A1}^{\sigma}(\mathbf{r},\mathbf{r}';\omega)+G_{A2}^{\sigma}(\mathbf{r},\mathbf{r}';\omega)$, which further gives (see more details in Refs. [38,39])

$$\begin{aligned}G_{A1}^{\sigma}&=\sum_{ijl,rst}(-1)^{r+s+t-q_\sigma}\frac{\cos kR_{ijl,rst}}{4\pi R_{ijl,rst}}\cdot\mathrm{erfc}(K_cR_{ijl,rst}),\\ G_{A2}^{\sigma}&=\sum_{ijl,rst}(-1)^{r+s+t-q_\sigma}\frac{\cos kR_{ijl,rst}}{4\pi R_{ijl,rst}}\cdot\mathrm{erf}(K_cR_{ijl,rst})\\ &=\sum_{\mathrm{npq}}\mathbb{A}_{\mathrm{npq}}^{\sigma}(\mathbf{r})\mathbb{A}_{\mathrm{npq}}^{\sigma}(\mathbf{r}')\cdot\Gamma^{(K_c)}(k,k_{\mathrm{npq}}).\end{aligned}\tag{15}$$

Here $\mathbf{k}\equiv(\mathrm{n}\pi/L_x,\,\mathrm{p}\pi/L_y,\,\mathrm{q}\pi/L_z)$ is the field mode index with $k_{\mathrm{npq}}:=|\mathbf{k}|$ and $\mathrm{n},\mathrm{p},\mathrm{q}\in\mathbb{Z}_0^+$. $R_{ijl,rst}:=|\mathbf{r}-\mathbf{R}'_{ijl,rst}|$ is the distance between the field point $\mathbf{r}$ and the image of $\mathbf{r}'\equiv(x',y',z')$ at

$$\begin{aligned}\mathbf{R}'_{ijl,rst}=&\,[2iL_x+(-1)^rx']\,\mathbf{e}_x+[2jL_y+(-1)^sy']\,\mathbf{e}_y\\&+[2lL_z+(-1)^tz']\,\mathbf{e}_z,\end{aligned}\tag{16}$$

with $i,j,l\in\mathbb{Z}$; $r,s,t=0,1$; and $q_{x,y,z}=r,s,t$. The function $\Gamma^{(K_c)}(k,k_{\mathrm{npq}})$ provides a fast-converging cutoff,

$$\Gamma^{(K_c)}(k,k_{\mathrm{npq}})=\frac{1}{2k_{\mathrm{npq}}}\left[\frac{e^{-\frac{(k+k_{\mathrm{npq}})^2}{4K_c^2}}}{k_{\mathrm{npq}}+k}+\frac{e^{-\frac{(k-k_{\mathrm{npq}})^2}{4K_c^2}}}{k_{\mathrm{npq}}-k}\right].$$

Here K_c is a free parameter [usually set as $K_c=\sqrt{\pi}/(2V^{1/3})$].

Now both the above G_{A1}^{σ} and G_{A2}^{σ} converge rapidly enough for numerical evaluations (in our numerical results below, $\sim10^3$ image terms are counted, see also the precision analysis in Refs. [38,39]). When $K_c\to 0$, the Green function $\tilde{\mathbb{G}}_A(\mathbf{r},\mathbf{r}';\omega)$ gives the form of image expansion, and when $K_c\to\infty$, $\tilde{\mathbb{G}}_A(\mathbf{r},\mathbf{r}';\omega)$ returns the form of mode expansion (13). In this sense, we say G_{A1}^{σ} and G_{A2}^{σ} indicate the contributions from the images and the mode propagation respectively. Then the dipolar interaction strength can be further obtained from Eqs. (8) and (10).

IV. NUMERICAL RESULTS

Based on the above discussions, now we consider the dipolar interaction between two magnetic dipoles inside a rectangular 3D cavity (with $L_{x,y,z}\equiv L$) given by Eq. (8). Without loss of generality, here we focus on the interaction term between two resonant transition dipoles, namely, the interaction term $V_{2\leftarrow 1}^{uv,ab}(\omega)\,\hat{\tau}_2^{uv}\hat{\tau}_1^{ab}$ as demonstrated in Fig. 1, so as to make a close comparison with the previous free-space results (1, 2) (the dipole frequency is set as $\omega\equiv 20\,cL^{-1}$). Hereafter we denote this interaction strength as $V_{2\leftarrow 1}^{\mathrm{cav}}$ for simplicity. The numerical results for different configurations are shown in Fig. 2.

In Figs. 2(a) and 2(b), dipole-1 (red) is placed at the center of the cavity, dipole-2 (green) moves from the center to the boundary ($\mathbf{r}_2=\mathbf{r}_1+R\,\mathbf{e}_x$ with $0<R<L_x/2$), and both dipoles are oriented in the z direction. As mentioned above, the full interaction contains the contributions from the field propagations in both ways $V_{1\leftrightarrow 2}^{\mathrm{cav}}=(V_{2\leftarrow 1}^{\mathrm{cav}}+V_{1\leftarrow 2}^{\mathrm{cav}})/2$, and clearly these two contributions $V_{2\leftarrow 1}^{\mathrm{cav}}(\omega)$ and $V_{1\leftarrow 2}^{\mathrm{cav}}(\omega)$ are not exactly the same as each other [Figs. 2(a) and 2(b)], which is different from the above isotropic situation in free space [Eq. (11)].

As a comparison, the dipolar interactions in free space with the same conditions are also presented [Eqs. (1) and (2), see the green and blue lines]. In the regime $\omega R/c>1$, the interaction $V_{2\leftarrow 1}^{\mathrm{cav}}$ exhibits significant oscillations with the distance R, which is more drastic than the free-space result $V(\omega)$ [see the dashed blue line and Eq. (2)]. When the distance between the two dipoles is quite small (in the regime $\omega R/c\ll 1$), $V_{2\leftarrow 1}^{\mathrm{cav}}$ just returns the static dipolar interaction in free space (1) with the power-law dependence $\sim R^{-3}$ [see the log-log scale inset in Fig. 2(a)]. That means, when the two dipoles are far from the conductor boundary, their interaction well returns the free-space situation [40], and this is also consistent with the situation in classical electrodynamics.

Accordingly, we consider the situation that the two dipoles are placed near the conductor plane. In Fig. 2(c), dipole-1 is set near the bottom center $\mathbf{r}_1=(0.5L_x,\,0.5L_y,\,0.01L_z)$, and still dipole-2 moves away from dipole-1 ($\mathbf{r}_2=\mathbf{r}_1+R\,\mathbf{e}_x$ with $0<R<L_x/2$). The dipole orientations are the same as those in Figs. 2(a) and 2(b). Again, in the short-distance regime, $V_{2\leftarrow 1}^{\mathrm{cav}}$ well returns the free-space result (1). But in the long-distance regime, it turns out the interaction $V_{2\leftarrow 1}^{\mathrm{cav}}$ is significantly suppressed compared with the free-space results (1) and (2). The reason is the dipole field $\hat{\mathbf{B}}_{\mathrm{d}1}(\mathbf{r})$ generated from dipole-1 should follow the boundary condition near the conductor plane during its propagation, thus $\hat{\mathbf{B}}_{\mathrm{d}1}(\mathbf{r})$ tends to be parallel with the conductor plane. Therefore, since here dipole-2 is perpendicular to the conductor plane, their local interaction $-\hat{\mathfrak{m}}_2\cdot\hat{\mathbf{B}}_{\mathrm{d}1}(\mathbf{r}_2)$ tends to vanish to zero [Eq. (8)].

Similar comparison is also made for two dipoles oriented in the x direction [Figs. 2(d) and 2(e)]. Since here the two dipoles are parallel to the conductor plane, there is no suppressing

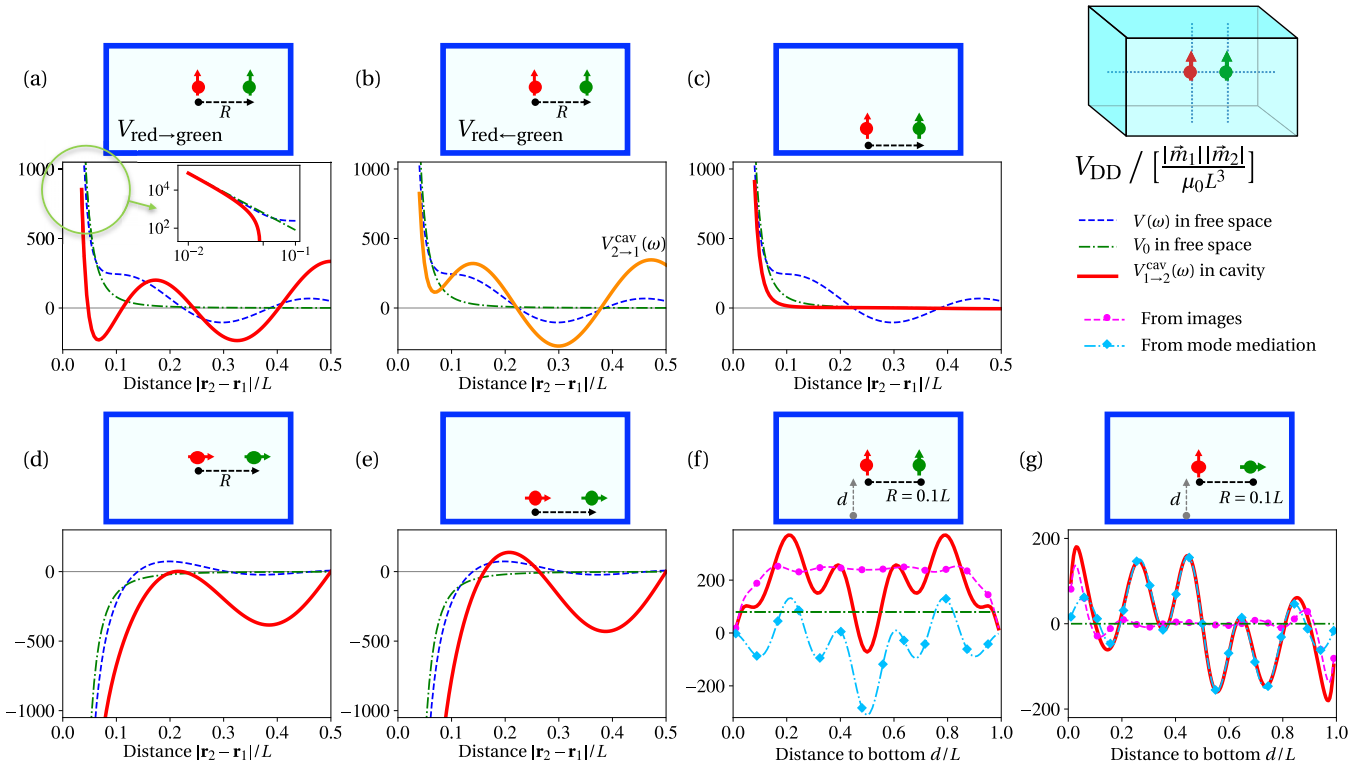

FIG. 2. The dipolar interaction in a rectangular 3D cavity (solid red). (a) Dipole-1 (red symbol on the left) is placed in the box center $\mathbf{r}_1 = (0.5L_x,\ 0.5L_y,\ 0.5L_z)$ with $L_{x,y,z} \equiv L$, and dipole-2 (green symbol on the right) is placed at $\mathbf{r}_2 = \mathbf{r}_1 + R\,\mathbf{e}_x$ as in all the other figures. Both $\vec{m}_{1,2}$ are oriented in the z direction, and the interaction $V_{2\leftarrow1}^{\text{cav}}(\omega)$ is generated between dipole-2 and the field from dipole-1, with $\omega/c = 20L^{-1}$. (b) All the conditions are the same as those in panel (a) except the interaction $V_{1\leftarrow2}^{\text{cav}}(\omega)$ is generated between dipole-1 and the field from dipole-2. (c) The two dipoles are placed near the bottom $\mathbf{r}_1 = (0.5L_x,\ 0.5L_y,\ 0.01L_z)$. (d) Both $\vec{m}_{1,2}$ are oriented in the x direction. (e) All the conditions are the same as those in panel (d) except the positions are the same as those in panel (c). (f) Both the two dipoles move from the bottom to the top, with $\mathbf{r}_1 = (0.5L_x,\ 0.5L_y,\ d)$, and the distance is fixed as $R = 0.1L$, and $0 < d < L_z$. Both $\vec{m}_{1,2}$ are oriented in the z direction. (g) All the conditions are the same as those in panel (f) except $\vec{m}_2$ is oriented in the x direction. In panels (f) and (g), the purple and blue lines indicate the contributions from the images and mode mediations, respectively. The dipolar interactions in free space are plotted for comparison, namely, V_0 in Eq. (1) (dot-dashed green line) and $V(\omega)$ in Eq. (2) (dashed blue line).

behavior as in Fig. 2(c) when the dipoles are placed near the cavity bottom, and the interactions $V_{2\leftarrow1}^{\text{cav}}$ in Figs. 2(d) and 2(e) look similar to each other.

To see this mechanism more clearly, we consider the distance between the two dipoles is fixed as $\mathbf{r}_2 = \mathbf{r}_1 + R\,\mathbf{e}_x$ with $R \equiv 0.1L$, and they both move from the cavity bottom to the top [$\mathbf{r}_1 = (0.5L_x,\ 0.5L_y,\ d)$ with $0 < d < L_z$ Fig. 2(f)], and clearly the interaction $V_{2\leftarrow1}^{\text{cav}}$ approaches zero when the two dipoles (in the z direction) approach the top and bottom boundaries. The contributions from the dipole images and the mode mediation are also presented respectively [from G_{A1}^{σ} and G_{A2}^{σ} in Eq. (15)], comparing with the free-space interaction strength, which is a constant due to the fixed distance. But if dipole-2 is oriented in the x direction, $V_{2\leftarrow1}^{\text{cav}}$ would remain nonzero at the boundaries $d \to 0,\ L_z$ [Fig. 2(g)].

The influence from the conductor boundary also can be understood from the demonstration in Fig. 1. When dipole-1 is placed near the conductor plane, the dipole field felt by dipole-2 comes from both dipole-1 and its image. In the bulk regime far from the boundaries [see Figs. 2(f) and 2(g)], the interaction strength exhibits significant oscillations varying with positions, which come from the spatial distribution of the mediating modes, especially the ones nearly resonant with the dipole frequency.

V. DISCUSSIONS

By properly considering the propagation of the dipole field, we obtain the full magnetic dipolar interaction which includes all the interaction terms between permanent dipoles, resonant or nonresonant transition dipoles, and even the counter-rotating interaction terms altogether. The result applies for general boundary conditions, which already have been enclosed in the tensor Green function $\tilde{\mathbb{G}}_A(\mathbf{r}, \mathbf{r}'; \omega)$, and this is also consistent with the classical Maxwell equation. In particular, we show the interaction for the dipolar interaction in a rectangular 3D cavity and how it is connected with previous results under certain conditions.

From the above results, it is worth noticing that the dipolar interaction exhibits significant dependence of three typical lengths, i.e., the distance R between the two dipoles, the distance d between the dipoles to the cavity boundaries, and the wavelength λ of the field modes nearly resonant with the dipole frequencies.

For example, the NV centers ($\omega_{\rm NV} \simeq 2.88$ GHz) in a nanodiamond interact with the ^{13}C nuclear spins ($\omega_{\rm C} \sim 1$ MHz) around the magnetic dipolar interaction [5,6,20]. If the nanodiamond is placed in the center of a 3D cavity whose base frequency is ∼1 GHz with the size ∼10 cm [41], the magnetic dipolar interaction between the NV center and the nuclear spins around it should be almost the same as the static dipolar interaction (1) in free space, since these magnetic dipoles are too far away from the cavity boundaries [Fig. 2(a)]. If the nanodiamond is placed quite near to the cavity boundary, or quite close to a metallic tip, their dipolar interactions would be significantly changed.

On the other hand, considering some cold atoms are placed in an optical cavity (usually ∼100 μm), the distance R between the flying atoms, their distance to the cavity boundaries d, and the cavity mode wavelength λ would be comparable [42–47]. In this case, the dipolar interaction in the cavity would have a complicated position dependence as shown in Fig. 2.

Throughout the discussion, the dynamics of the mediating dipole field is simply described by the Maxwell equation and the corresponding Green function. Thus, by properly changing to some other field equations, this approach can be generalized to study the interaction mediated by other kinds of fields, such as the exciton-polariton field or the phonon field [15,24,48,49].

In the above discussions about the cavity situation, we focus only on the ideal conductors, and realistic situations may involve more physical effects. For example, near the metal surface, the surface plasmon induced by the electron density oscillation would influence the EM field nearby, and that would bring in extra changes to our above discussions [16,24]. In principle, the interaction induced by these extra fields also can be considered by the approach in this paper.

ACKNOWLEDGMENTS

S.-W.L. greatly appreciates the helpful discussion with N. Wu, D. Xu, and B. Zhang at BIT. This study is supported by the NSF of China (Grant No. 11905007), the funding from Ministry of Science and Technology of China (Grant No. 2021YFE0193500), and the Beijing Institute of Technology Research Fund Program for Young Scholars.

APPENDIX A: THE EFFECTIVE INTERACTION MEDIATED BY ONE FIELD MODE

We consider that two dipoles both interact with one common field mode, and the Hamiltonian of the three-body system is $\hat{H} = \hat{H}_0 + \hat{V}$, where

$$\begin{aligned} \hat{H}_0 &= \omega_1 \hat{\tau}_1^+ \hat{\tau}_1^- + \omega_2 \hat{\tau}_2^+ \hat{\tau}_2^- + \nu \hat{a}^\dagger \hat{a}, \\ \hat{V} &= g_1 \hat{\tau}_1^+ \hat{a} + g_2 \hat{\tau}_2^+ \hat{a} + \text{H.c.} \end{aligned} \tag{A1}$$

The Fröhlich-Nakajima canonical transformation gives an effective Hamiltonian [26,27],

$$\begin{aligned} \hat{H}_{\rm eff} &= e^{-\hat{S}} \hat{H} e^{\hat{S}} = \hat{H} + [\hat{H}, \hat{S}] + \tfrac{1}{2}[\hat{H}, [\hat{H}, \hat{S}]] + \cdots \\ &\simeq \hat{H}_0 + \tfrac{1}{2}[\hat{V}, \hat{S}], \end{aligned} \tag{A2}$$

where the first order $\hat{V} + [\hat{H}_0, \hat{S}] \equiv 0$ is eliminated by properly setting $\hat{S} := A\hat{\tau}_1^+ \hat{a} + B\hat{\tau}_2^+ \hat{a} - \text{H.c.}$, and that gives

$$\begin{aligned} &[\hat{H}_0, \hat{S}] = (\omega_1 - \nu)(A\hat{\tau}_1^+ \hat{a} + \text{H.c.}) + (\omega_2 - \nu)(B\hat{\tau}_2^+ \hat{a} + \text{H.c.}), \\ &\Rightarrow A = \frac{g_1}{\nu - \omega_1}, \quad B = \frac{g_2}{\nu - \omega_2}. \end{aligned} \tag{A3}$$

Therefore, the effective interaction becomes

$$\begin{aligned} \hat{V}_{\rm eff} &= \frac{1}{2}[\hat{V}, \hat{S}] = (\tilde{\beta} \hat{\tau}_1^+ \hat{\tau}_2^- + \text{H.c.}) + \sum_{\alpha=1,2} \tilde{\xi}_\alpha \hat{\tau}_\alpha^z \left(\hat{a}^\dagger \hat{a} + \frac{1}{2} \right) \\ \tilde{\beta} &= \frac{1}{2}\left[\frac{g_1 g_2^*}{\omega_1 - \nu} + \frac{g_2 g_1^*}{\omega_2 - \nu} \right], \quad \tilde{\xi}_\alpha = \frac{|g_\alpha|^2}{\omega_\alpha - \nu}. \end{aligned} \tag{A4}$$

The first term in $\hat{V}_{\rm eff}$ eliminates the mediating field mode and gives the interchange interaction between the two dipoles as shown in Eq. (3), while the second term can be regarded as a correction to the self-Hamiltonian $\omega_\alpha \hat{\tau}_\alpha^+ \hat{\tau}_\alpha^-$ which depends on the mode state.

APPENDIX B: THE DYNAMICAL EQ. (4) FOR THE QUANTIZED MAGNETIC FIELD

Here we show how Eq. (4) for the quantized magnetic field $\hat{\mathbf{B}}(\mathbf{r}, t)$ is derived. We consider one magnetic dipole at position $\mathbf{r}_1$ interacting with the EM field, and the full dynamics of this system is described by $\hat{\mathcal{H}} = \hat{H}_1 + \hat{V}_1 + \hat{H}_{\rm EM}$, where $\hat{H}_1$ is the self-Hamiltonian of the magnetic dipole, and

$$\begin{aligned} \hat{H}_{\rm EM} &= \int d^3\mathbf{x} \left[\frac{1}{2}\epsilon_0 \hat{\mathbf{E}}^2(\mathbf{x}) + \frac{1}{2\mu_0} \hat{\mathbf{B}}^2(\mathbf{x}) \right], \\ \hat{V}_1 &= -\hat{\mathbf{m}} \cdot \hat{\mathbf{B}}(\mathbf{r}_1) \end{aligned} \tag{B1}$$

are the Hamiltonian of the EM field and the local interaction between the magnetic dipole and the magnetic field, respectively. Under the Coulomb gauge, the quantized electric and magnetic field operators read [37]

$$\begin{aligned} \hat{\mathbf{E}}(\mathbf{r}, t) &= \sum_{\mathbf{k}\varsigma} \sqrt{\frac{\hbar\omega_k}{2\epsilon_0 V}} \mathbf{e}_{\mathbf{k}\varsigma} [i e^{i\mathbf{k}\cdot\mathbf{r}} \hat{a}_{\mathbf{k}\varsigma}(t) - \text{H.c.}], \\ \hat{\mathbf{B}}(\mathbf{r}, t) &= \sum_{\mathbf{k}\varsigma} \sqrt{\frac{\hbar\omega_k}{2\epsilon_0 V}} \frac{\mathbf{e}_{\mathbf{k}} \times \mathbf{e}_{\mathbf{k}\varsigma}}{c} [i e^{i\mathbf{k}\cdot\mathbf{r}} \hat{a}_{\mathbf{k}\varsigma}(t) - \text{H.c.}], \end{aligned} \tag{B2}$$

where $\mathbf{e}_{\mathbf{k}\varsigma}$ denotes the two polarization directions perpendicular to the wave vector $\mathbf{k}$. These quantized field operators follow the Heisenberg equation $\partial_t \hat{o} = \frac{1}{i\hbar}[\hat{o}, \hat{\mathcal{H}}]$, and that gives

$$\partial_t \hat{\mathbf{B}}(\mathbf{r}) = \frac{1}{i\hbar}[\hat{\mathbf{B}}(\mathbf{r}), \hat{\mathcal{H}}] = -\nabla \times \hat{\mathbf{E}}, \tag{B3a}$$

$$\partial_t \hat{\mathbf{E}}(\mathbf{r}) = c^2[\nabla \times \hat{\mathbf{B}} - \mu_0 \nabla \times \hat{\mathbf{m}} \delta(\mathbf{r} - \mathbf{r}_1)]. \tag{B3b}$$

To obtain this result, the following commutation relations are calculated:

$$\begin{aligned} &[\hat{\mathbf{E}}(\mathbf{r}), \ \hat{\mathbf{m}} \cdot \hat{\mathbf{B}}(\mathbf{r}_1)] \\ &= \sum_{\mathbf{k}\varsigma, \mathbf{q}\sigma} \frac{-\hbar\sqrt{\omega_k \omega_q}}{2\epsilon_0 V c} \mathbf{e}_{\mathbf{k}\varsigma} (\hat{\mathbf{m}} \cdot \mathbf{e}_{\mathbf{q}} \times \mathbf{e}_{\mathbf{q}\sigma}) \\ &\quad \times [e^{i\mathbf{k}\cdot\mathbf{r}} \hat{a}_{\mathbf{k}\varsigma} - e^{-i\mathbf{k}\cdot\mathbf{r}} \hat{a}_{\mathbf{k}\varsigma}^\dagger, \ e^{i\mathbf{q}\cdot\mathbf{r}_1} \hat{a}_{\mathbf{q}\sigma} - e^{-i\mathbf{q}\cdot\mathbf{r}_1} \hat{a}_{\mathbf{q}\sigma}^\dagger] \end{aligned}$$

$$= \sum_{\mathbf{k}\varsigma} \frac{-\hbar\omega_k}{2\epsilon_0 V c}(\hat{\mathbf{m}}\cdot\mathbf{e}_\mathbf{k}\times\mathbf{e}_{\mathbf{k}\varsigma})\mathbf{e}_{\mathbf{k}\varsigma}[e^{-i\mathbf{k}\cdot(\mathbf{r}-\mathbf{r}_1)} - e^{i\mathbf{k}\cdot(\mathbf{r}-\mathbf{r}_1)}]$$

$$= \sum_{\mathbf{k}} \frac{\hbar}{2\epsilon_0 V}\,\mathbf{k}\times\hat{\mathbf{m}}[e^{-i\mathbf{k}\cdot(\mathbf{r}-\mathbf{r}_1)} - e^{i\mathbf{k}\cdot(\mathbf{r}-\mathbf{r}_1)}]$$

$$= \frac{i\hbar}{\epsilon_0}\nabla_\mathbf{r}\times[\hat{\mathbf{m}}\delta(\mathbf{r}-\mathbf{r}_1)], \tag{B4}$$

$$[\hat{\mathbf{E}}(\mathbf{r}),\ \hat{\mathbf{B}}^2(\mathbf{x})] = \frac{2i\hbar}{\epsilon_0}\nabla_\mathbf{r}\times[\hat{\mathbf{B}}(\mathbf{x})\delta(\mathbf{r}-\mathbf{x})]. \tag{B5}$$

In the above calculations, we used the relations $\sum_{\varsigma=1,2}\mathbf{e}_{\mathbf{k}\varsigma}\mathbf{e}_{\mathbf{k}\varsigma} = \mathbf{1} - \mathbf{e}_\mathbf{k}\mathbf{e}_\mathbf{k}$, and $\hat{\mathbf{m}}\cdot\mathbf{k}\times\mathbf{1} = -\mathbf{k}\times\hat{\mathbf{m}}$.

Notice that Eqs. (B3a) and (B3b) and the current term $\nabla\times[\hat{\mathbf{m}}\delta(\mathbf{r}-\mathbf{r}_1)] := \hat{\mathbf{J}}$ have the same form as the classical Maxwell equations [19]. Taking the curl of Eq. (B3b) gives the dynamical equation (4) for the quantized magnetic field $\hat{\mathbf{B}}(\mathbf{r},t)$ in the main text, which has the same form as the classical electrodynamics. Indeed, during the canonical quantization of the EM field, the equations of motion for the quantized operators should keep the same form as their classical counterparts, which roots from the consistency from the classical Poisson bracket to the quantum commutator $\{A,B\}\to\frac{1}{i\hbar}[\hat{A},\hat{B}]$.

APPENDIX C: EIGENMODES IN THE RECTANGULAR CAVITY

Here we show the eigenmodes of the cavity field given by $[\nabla^2+\mathbf{k}^2]\vec{\mathtt{A}}_\mathbf{k}(\mathbf{r}) = 0$ in the rectangular region $x,y,z\in[0,L_{x,y,z}]$. The boundary condition requires $\hat{n}\times\vec{\mathtt{A}}_\mathbf{k}(\mathbf{r}) = 0$ and $\nabla\cdot\vec{\mathtt{A}}_\mathbf{k}(\mathbf{r}) = 0$ for $\mathbf{r}$ on the boundary planes. Denoting the vector eigenmodes as $\vec{\mathtt{A}}_\mathbf{k}(\mathbf{r}) := (\mathtt{A}^x_{\mathrm{npq}},\ \mathtt{A}^y_{\mathrm{npq}},\ \mathtt{A}^z_{\mathrm{npq}})$, the eigenmodes read [38,39] as follows:

$$\mathtt{A}^x_{\mathrm{npq}}(\mathbf{r}) = \sqrt{\frac{4(2-\delta_{\mathrm{n0}})}{V}}\cos\frac{\mathrm{n}\pi}{L_x}x\sin\frac{\mathrm{p}\pi}{L_y}y\sin\frac{\mathrm{q}\pi}{L_z}z,$$

$$\mathtt{A}^y_{\mathrm{npq}}(\mathbf{r}) = \sqrt{\frac{4(2-\delta_{\mathrm{p0}})}{V}}\sin\frac{\mathrm{n}\pi}{L_x}x\cos\frac{\mathrm{p}\pi}{L_y}y\sin\frac{\mathrm{q}\pi}{L_z}z,$$

$$\mathtt{A}^z_{\mathrm{npq}}(\mathbf{r}) = \sqrt{\frac{4(2-\delta_{\mathrm{q0}})}{V}}\sin\frac{\mathrm{n}\pi}{L_x}x\sin\frac{\mathrm{p}\pi}{L_y}y\cos\frac{\mathrm{q}\pi}{L_z}z,$$

where $\mathbf{k}_{\mathrm{npq}} = (\mathrm{n}\pi/L_x,\ \mathrm{p}\pi/L_y,\ \mathrm{q}\pi/L_z)$ and $\mathrm{n},\mathrm{p},\mathrm{q}\in\mathbb{Z}_0^+$. Here $\mathtt{A}^\sigma_{\mathrm{npq}}(\mathbf{r})$ are normalized as $\int_V \mathtt{A}^\sigma_\mathbf{k}(\mathbf{r})\,\mathtt{A}^\varsigma_\mathbf{q}(\mathbf{r})\,d^3r = \delta_{\sigma\varsigma}\delta_{\mathbf{kq}}$.

[1] J. M. Martinis, K. B. Cooper, R. McDermott, M. Steffen, M. Ansmann, K. D. Osborn, K. Cicak, S. Oh, D. P. Pappas, R. W. Simmonds, and C. C. Yu, Phys. Rev. Lett. **95**, 210503 (2005).

[2] H. Paik, D. I. Schuster, L. S. Bishop, G. Kirchmair, G. Catelani, A. P. Sears, B. R. Johnson, M. J. Reagor, L. Frunzio, L. I. Glazman, S. M. Girvin, M. H. Devoret, and R. J. Schoelkopf, Phys. Rev. Lett. **107**, 240501 (2011).

[3] C. Rigetti, J. M. Gambetta, S. Poletto, B. L. T. Plourde, J. M. Chow, A. D. Córcoles, J. A. Smolin, S. T. Merkel, J. R. Rozen, G. A. Keefe, M. B. Rothwell, M. B. Ketchen, and M. Steffen, Phys. Rev. B **86**, 100506(R) (2012).

[4] J. Lisenfeld, A. Bilmes, S. Matityahu, S. Zanker, M. Marthaler, M. Schechter, G. Schön, A. Shnirman, G. Weiss, and A. V. Ustinov, Sci. Rep. **6**, 23786 (2016).

[5] M. W. Doherty, N. B. Manson, P. Delaney, F. Jelezko, J. Wrachtrup, and L. C. L. Hollenberg, Phys. Rep. **528**, 1 (2013).

[6] N. Zhao, S.-W. Ho, and R.-B. Liu, Phys. Rev. B **85**, 115303 (2012).

[7] S. Yang, D. Z. Xu, Z. Song, and C. P. Sun, J. Chem. Phys. **132**, 234501 (2010).

[8] R. El-Ganainy and S. John, New J. Phys. **15**, 083033 (2013).

[9] H. Dong, S.-W. Li, Z. Yi, G. S. Agarwal, and M. O. Scully, arXiv:1608.04364.

[10] N. J. Lambert, J. A. Haigh, S. Langenfeld, A. C. Doherty, and A. J. Ferguson, Phys. Rev. A **93**, 021803(R) (2016).

[11] D. G. Baranov, R. S. Savelev, S. V. Li, A. E. Krasnok, and A. Alù, Laser & Photonics Reviews **11**, 1600268 (2017).

[12] Z. Liao, H. Nha, and M. S. Zubairy, Phys. Rev. A **94**, 053842 (2016).

[13] E. Shahmoon and G. Kurizki, Phys. Rev. A **87**, 062105 (2013).

[14] M. Donaire, J. M. Muñoz-Castañeda, and L. M. Nieto, Phys. Rev. A **96**, 042714 (2017).

[15] C. L. Cortes and Z. Jacob, Nat. Commun. **8**, 14144 (2017).

[16] L.-P. Yang, C. Khandekar, T. Li, and Z. Jacob, New J. Phys. **22**, 023037 (2020).

[17] A. Gonzalez-Tudela, D. Martin-Cano, E. Moreno, L. Martin-Moreno, C. Tejedor, and F. J. Garcia-Vidal, Phys. Rev. Lett. **106**, 020501 (2011).

[18] L. Ying, M. Zhou, M. Mattei, B. Liu, P. Campagnola, R. H. Goldsmith, and Z. Yu, Phys. Rev. Lett. **123**, 173901 (2019).

[19] J. D. Jackson, *Classical Electrodynamics*, 3rd ed. (Wiley, New York, 1998).

[20] J. Wrachtrup and F. Jelezko, J. Phys.: Condens. Matter **18**, S807 (2006).

[21] R. H. Lehmberg, Phys. Rev. A **2**, 883 (1970).

[22] G. S. Agarwal, *Quantum Statistical Theories of Spontaneous Emission and Their Relation to Other Approaches* (Springer, Berlin, 1974).

[23] Z. Ficek and R. Tanaś, Phys. Rep. **372**, 369 (2002).

[24] J. C. G. Henriques, B. Amorim, and N. M. R. Peres, Phys. Rev. B **103**, 085407 (2021).

[25] V. N. Shatokhin, M. Walschaers, F. Schlawin, and A. Buchleitner, New J. Phys. **20**, 113040 (2018).

[26] H. Fröhlich, Phys. Rev. **79**, 845 (1950).

[27] S. Nakajima, Adv. Phys. **4**, 363 (1955).

[28] S.-W. Li, L.-P. Yang, and C.-P. Sun, Eur. Phys. J. D **68**, 45 (2014).

[29] E. V. Goldstein and P. Meystre, Phys. Rev. A **56**, 5135 (1997).

[30] J. Wang, H. Dong, and S.-W. Li, Phys. Rev. A **97**, 013819 (2018).

[31] F.-q. Hu, Q. Zhao, and S.-W. Li, J. Phys. B **53**, 065003 (2020).

[32] C.-T. Tai, *Dyadic Green Functions in Electromagnetic Theory*, 2nd ed. (IEEE Press, Piscataway, NJ, 1994).

[33] H. T. Dung, L. Knöll, and D.-G. Welsch, Phys. Rev. A **66**, 063810 (2002).

[34] B. Huttner and S. M. Barnett, Phys. Rev. A **46**, 4306 (1992).

[35] S. Scheel, L. Knöll, and D.-G. Welsch, Phys. Rev. A **58**, 700 (1998).
[36] S. Scheel and D.-G. Welsch, Phys. Rev. Lett. **96**, 073601 (2006).
[37] W. Vogel and D.-G. Welsch, *Quantum Optics*, 3rd ed. (Wiley-VCH, Weinheim, 2006).
[38] M. Park, IEEE Microwave Wireless Compon. Lett. **19**, 260 (2009).
[39] M. Sanamzadeh and L. Tsang, Prog. Electromagn. Res. C **96**, 243 (2019).
[40] G. S. Agarwal and S. Dutta Gupta, Phys. Rev. A **57**, 667 (1998).
[41] J. R. Ball, Y. Yamashiro, H. Sumiya, S. Onoda, T. Ohshima, J. Isoya, D. Konstantinov, and Y. Kubo, Appl. Phys. Lett. **112**, 204102 (2018).
[42] Y. Tang, W. Kao, K.-Y. Li, and B. L. Lev, Phys. Rev. Lett. **120**, 230401 (2018).
[43] P. M. Lushnikov, Phys. Rev. A **66**, 051601(R) (2002).
[44] A. Griesmaier, J. Stuhler, T. Koch, M. Fattori, T. Pfau, and S. Giovanazzi, Phys. Rev. Lett. **97**, 250402 (2006).
[45] M. Fattori, G. Roati, B. Deissler, C. D'Errico, M. Zaccanti, M. Jona-Lasinio, L. Santos, M. Inguscio, and G. Modugno, Phys. Rev. Lett. **101**, 190405 (2008).
[46] E. J. Davis, G. Bentsen, L. Homeier, T. Li, and M. H. Schleier-Smith, Phys. Rev. Lett. **122**, 010405 (2019).
[47] R. G. DeVoe and R. G. Brewer, Phys. Rev. Lett. **76**, 2049 (1996).
[48] J. D. A. Espinoza, M. Mazzanti, K. Fouka, R. X. Schüssler, Z. Wu, P. Corboz, R. Gerritsma, and A. Safavi-Naini, Phys. Rev. A **104**, 013302 (2021).
[49] Y.-G. Huang, G. Chen, C.-J. Jin, W. M. Liu, and X.-H. Wang, Phys. Rev. A **85**, 053827 (2012).